JTTEE5 9:181-190

Quality Control of Thermal Barrier Coatings Using Acoustic Emission

David J. Andrews and Jenifer A.T. Taylor

(Submitted 26 January 1999; in revised form 6 December 1999)

Thermal barrier coatings (TBCs) are used to protect underlying metal from heat generated during combustion of fuel, especially in truck engines and jet turbines. These coatings are thin, partially stabilized zirconia, separated from the substrate metal by an interface layer, which serves to enhance bonding and reduce the thermal expansion mismatch between the metal and the ceramic. The reliability of these coatings is currently not predictable.

The work described in this paper focused on the use of acoustic emission (AE) as a quality control test for TBCs. The test specimens were commercially sprayed straps. The data show that differences in spraying parameters and microstructure are clearly visible in the emissions during thermal cycling. This work indicates that the failure mechanism can be predicted from the AEs during the first thermal cycle.

Keywords thermal barrier coatings, nondestructive test, acoustic emission, zirconia

1. Introduction

The focus of this research project is the characterization of plasma-sprayed thermal barrier coatings (TBCs) using acoustic emission (AE) as a nondestructive evaluation technique. A limiting factor in the industrial use of TBCs is inconsistent coating quality. Thousands of cycles of life are expected from TBCs, but failure can occur in under 20 cycles.[1] The current status of coating evaluation in industry is visual inspection followed by an engine test. If a failure occurs, loose pieces of the coating will cause damage to engine components. Nondestructive evaluation is desirable to avoid these expensive and time-consuming proof tests.[2]

The ultimate goal of the project is to develop a nondestructive test of plasma-sprayed TBCs for diesel-engine pistons. This initial work was accomplished with commercially sprayed test straps, a much simpler geometry than pistons. Acoustic emission signals were correlated to failure mechanisms and processing differences through characterization of the TBCs at various stages in the thermal cycling process.

1.1 Thermal Barrier Coatings

Refractory ceramics are used as TBCs to protect the underlying metal from the high temperature in the combustion gas, which can reach levels above the softening point of the alloy. Desirable property characteristics for TBCs are low thermal conductivity, high thermal expansion coefficient, low stiffness, and thermodynamic and mechanical stability. Plasma-sprayed yttria-stabilized zirconia (YSZ) is commonly the material of choice in such applications. A bond coat is used to reduce the thermal-expansion mismatch between the top coat and the substrate.[3]

David J. Andrews and **Jenifer A.T. Taylor,** NYS College of Ceramics at Alfred University, Alfred, NY 14802.

A mechanical model showing the impact and residual stress behavior has been developed[4] that describes, in general, the deposition of coatings during the plasma spray process. Assumptions made in the model are that the impinging particles are completely molten and the substrate is massive and rigid when compared to the deposited splats. An additional assumption is that the heat from the molten particles is transferred to the substrate and quickly dissipated, approximating steady-state temperature conditions. The particle quenches rapidly and is assumed to be well bonded and continuous upon cooling.

The particle cannot relax to an equilibrium configuration, because it is constrained by the substrate and the quenching rate is very rapid (10^4 to 10^6 K/s).[4] Since it is forced to remain in a stretched condition, the particle experiences a residual tensile stress due to deposition, referred to as a quenching stress in the literature.[4] This stress is often high enough to cause microcracking in brittle materials.[5,6]

Substrate temperature influences the residual mechanical stresses. The thermal expansion coefficient of the YSZ is about half that of the bond coat.[3] When the coating/substrate composite cools after deposition, a residual stress component arises, which is always compressive because the coating is not contracting as much as the substrate. A hotter substrate will result in a larger compressive stress.

Residual compressive stresses are reported to be quite detrimental, because there is an induced tensile stress perpendicular to the plane of the coating, which causes debonding.[7] At lower substrate temperatures, the tensile stresses are higher, but these stresses remain in the plane of the coating and tend to induce microcracking (for brittle materials) during deposition. A higher density of such cracks provides a toughening effect, because they arrest cracks that are propagating through the plane of the coating.

Tensile and compressive stresses alternate in the coating during the upshock and downshock portions of the thermal shock cycle, respectively, as the coating and substrate are heated and cooled. According to this work, the largest temperature gradient in the specimens occurs in the first minute of the upshock. Substrate temperature was measured by spot welding a thermocouple

on the top side of the substrate. The temperature increases rapidly, as shown in Table 1.

An approximate tensile stress in the coating was calculated using the formula

$$\sigma = E\Delta\alpha\Delta T$$

where σ is the stress, E is Young's modulus of the coating, α is the difference in thermal expansion between the coating and substrate, and T is the temperature difference over a given time. The stresses in the first minute are calculated to be on the order of 250 MPa for these specimens. Stresses of this magnitude will cause cracking during the upshock, as will be shown by AE data presented later. A stress of similar magnitude will arise in compression during the downshock. Since the most extensive cracking occurred in the initial upshock, it is thought that the actual compressive stresses are minimized due to the freedom of the microstructure to contract. Therefore, the contention made here is that the AEs on the upshock are the more important events, since they describe the extent of the damage in the microstructure.

1.2 Acoustic Emission

Acoustic emission is a transient elastic wave that is created by energy released from the microstructure of a material, which is under stress.[8,9] As a crack is initiated and propagates through a material, measurable characteristics of the AEs from this event reveal details about the microstructure that are not obvious on visual inspection. The AE signals can be placed in two broad categories: continuous and burst-type emissions. Continuous emission is typically generated by plastic deformation mechanisms such as multiple dislocation slip.[9] Burst-type emission can result from microcracking in brittle materials, fracture of hard inclusions in alloys, phase transformations, fibers debonding from a matrix, or any other discrete fracture process.[9,10] (Details of AE analysis are given in the Appendix.)

Partially stabilized zirconia has been studied in both the monolithic and plasma-sprayed forms. Konsztowicz and his coworkers performed thermal shock tests of magnesia-partially-stabilized zirconia refractory bars.[11,12] The tests were performed at varying thermal shock loads (200 °C < T < 900 °C) with AE measured upon quenching in silicone oil. Through strength tests and microscopy, microcracking at the grain boundaries was attributed to low-amplitude hits. Large-amplitude events (>53 dB) were attributed to transgranular fracture.

Table 1 Approximate substrate temperatures during the first 2 min of the upshock

Time (s)	Temperature (°C)
Start	23
15	230
30	355
45	465
60	555
75	625
90	675
105	710
120	738

Acoustic emission measurements on plasma-sprayed zirconia have been discussed in terms of the cumulative counts from the sample. Shankar *et al.*[1] have performed thermal shock tests, which have shown an AE dependency with respect to coating preparation condition. Samples with no bond coat showed relatively low AE activity for every thermal shock cycle. Those with a bond coat exhibited much greater initial AE activity, which then dropped off for subsequent cycles. It was suggested that this drop off indicated formation of a stable microcrack network.[1] Berndt and Herman have focused on the count-rate distribution in an effort to distinguish cracking mechanisms during their tests.[13] They proposed that count rate, the number of counts measured in a given time frame (1 min), is an indication not only of the extent of cracking, but of the cracking mechanism as well. The AE data were measured from plasma-sprayed rods on the downshock portion of the cycle. They were able to establish trends, when comparing peak count rates at a given temperature, for different processing conditions. The trends were a function of the residual stresses and the microstructural condition in the as-sprayed coatings.

Trends in AE data are used to describe the deformation processes for a given material. Amplitude distribution analyses, that is, the total number of hits at various amplitudes, are one useful trend. Pollock has summarized four amplitude distribution analyses that may be appropriately applied to AE data.[9] The model applied to this work is a cumulative distribution function known as the power law.[14] Assumptions of this technique are that the AE response will be burst-type emission,[9] and that frequency-dependent attenuation is negligible.[15]

Stated as an equation, the power law is

$$F(A) = (A/A_t)^{-b}$$

where A is the amplitude for a given hit, A_t is the threshold setting, $F(A)$ is the number of hits with amplitude greater than A, and b is the slope of the curve on log-log axes. After collecting the AE data, the unknown in this equation is b. The magnitude of the b parameter is considered to be a description of the type of fracture mechanism in the material, which typically ranges between 0.4 and 4 (decades/decade).[9] A high b value indicates many hits just above the threshold with a lack of high-amplitude events. Lower b values indicate a larger proportion of events of higher amplitude. The b parameter is useful because it is fairly independent of thickness. A greater number of events would increase the number of counts but not change the amplitude distribution, which determines the slope on a log/log graph.

Acoustic emission sources, which can be expected in plasma-sprayed zirconia, are microcracking, phase transformations, and macrocracking. Assuming that a single event corresponds to a single source (neglecting signal interference), then the amplitude of an AE event is related to the change in size of an isolated source. Microcraking and phase transformations are localized (within a splat) events, which are expected to release relatively small bursts of energy. These sources would then produce low-amplitude events. Macrocracking, conversely, is indicative of fracture on a larger scale, such as delamination of the coating from the substrate or crack propagation through the bulk of the coating. Examples of these types of macrocracking are shown in Fig. 1 and 2.

Considering the application of amplitude distributions to the AE data, the magnitude of the b parameter should be an indica-

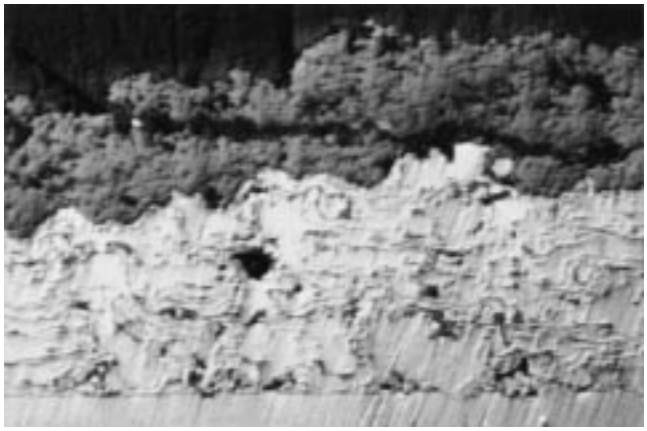

Fig. 1 Horizontal crack propagation through the bulk of the YSZ top coat. (The coating thickness is approximately 300 mm.)

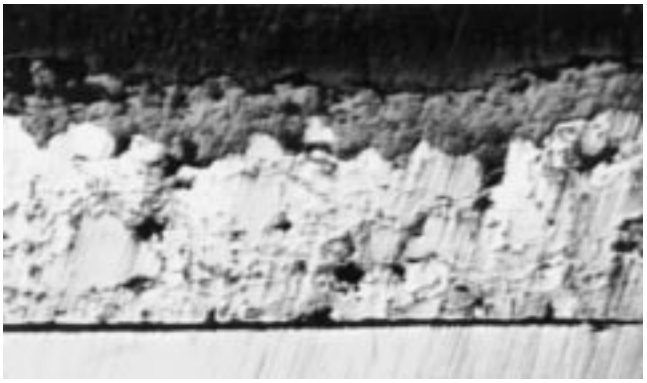

Fig. 2 Delamination of the bond coat from the substrate. (The coating thickness is approximately 300 mm.)

tion of the dominant mode of cracking. Previous AE researchers have made use of cumulative amplitude distributions. Holt *et al*. were able to correlate the amplitude distribution to the size distribution of pearlite colonies in steel.[9] Applications in composites testing attributed three distinct source mechanisms to the amplitude distribution of the data.[16] Pollock also reported tests that showed great distinction between brittle cracking ($0.7 < b < 1.5$) and plastic deformation ($b = 4.2$) in various alloys.[16] In the context of this work, with plasma-sprayed, yttria-stabilized zirconia, larger b values should indicate a predominance of microcracking and phase transformations. Higher energy events such as macrocracking and delamination would produce higher amplitude hits, yielding smaller b values.

2. Experimental Procedures

2.1 Samples

Three sets of samples were commercially sprayed at Heany Industries (Scottsville, NY). Nickel-chromium alloy straps that measured $300 \times 25 \times 2$ mm were used as substrates. A Metco 461 NS NiCoCrAlY bond coat was used in conjunction with a Metco 204 NS yttria (8 wt.%) partially stabilized zirconia top coat (Sulzer Metco, Westbury, NY). The coating covered an approximate area of 100×25 mm on one end of the strap. All the spraying was performed in an air atmosphere, using argon and hydrogen as the plasma constituents and argon as the powder carrier gas. Four different spraying conditions were used as a basis for comparing AEs. Normal conditions refer to coatings deposited with all the standard specifications that Heany uses on a day-to-day basis. The other three cases, torch too close, bond coat too thin, and top coat too thick, refer to common thermal spray parameter changes in the TBC deposition process. For these groups, the parameter mentioned was changed (*i.e.*, the plasma torch was positioned closer to the substrate than normal), and all other parameters remained unchanged with respect to the normal spraying conditions.

Experimental Setup. Thermal shock tests were performed on the sprayed samples. The AE was measured by clamping a high-temperature piezoelectric transducer (PAC D9215) on the unsprayed end of the strap, used in conjunction with a PAC 1220a preamplifier (Physical Acoustics Corporation, Princeton, NY). It should be noted that electrical insulation was wrapped around the ends of the clamp to prevent the existence of a short circuit between the sensor casing and the substrate. This is recommended practice to eliminate electrical noise from the system.[9]

The strap and transducer arrangement was held in place with a ring stand and clamp, while a tube furnace at 1000 °C was rolled onto the strap to provide the thermal shock effect. A schematic of the experimental setup is shown in Fig. 3. The AE data were read during both the heatup and quenching stages.

2.2 Characterization

Microstructural characterization was performed *via* optical (Reichert-Jung PolyVar Met, Vienna) and scanning electron microscopy (Amray 1810 SEM, Bedford, MA), and phase identification was performed using a parallel-beam X-ray diffractometer (Siemens Kristalloflex 810, Munich). Surface views of the coatings were seen best in the SEM due to the excellent depth of focus of this instrument.

Parallel-beam X-ray diffraction was used to provide phase identification of the coatings in as-sprayed and post-thermal-shock conditions. This technique was necessary because the texture (grain orientation - columnar grains) in the lamellae did not lend itself well to the ordinary diffraction machines. Theta/two-theta step scans were performed using a fixed theta angle of 2°, a step size of 0.05°, and a hold time of 5 s, allowing detection of 0.5 vol.% zirconia of different phases.

3. Results

3.1 Microstructure

The literature has suggested that residual stresses in plasma-sprayed ceramic coatings tend to be quite low due to formation of microcracks upon deposition.[11] Also described in some detail are the effects of changing the effective spraying temperature, the stand-off distance, and the presence of a bond coat. The mechanical models and changes in coating quality, due to the changes in spraying parameters, can be directly related to the samples used in this research. To this end, the coatings sprayed under normal

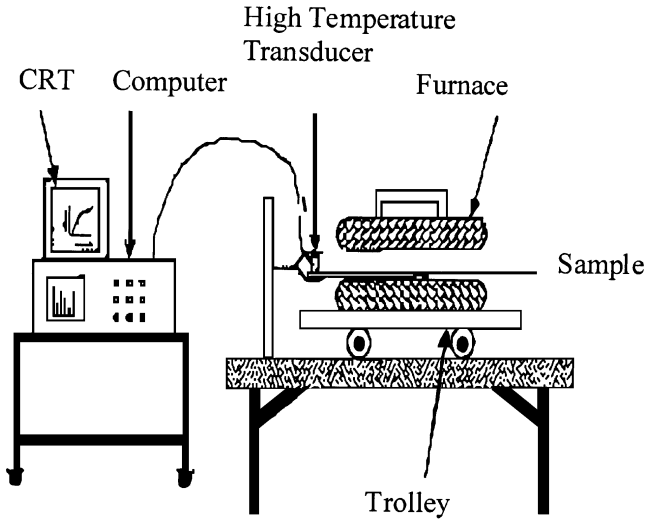

Fig. 3 Schematic of experimental setup for collecting AE data from thermal shock tests on plasma-sprayed YSZ

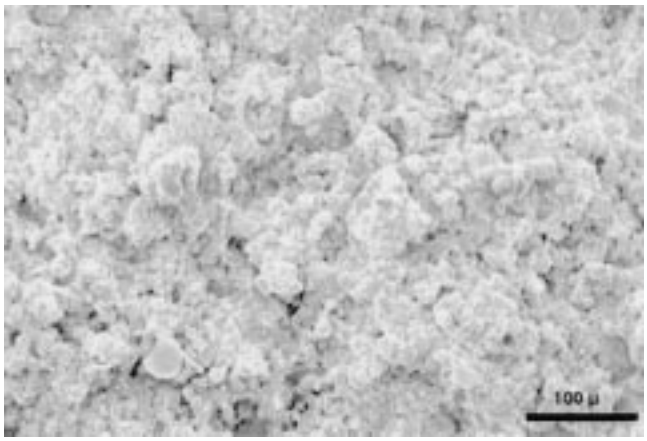

(a)

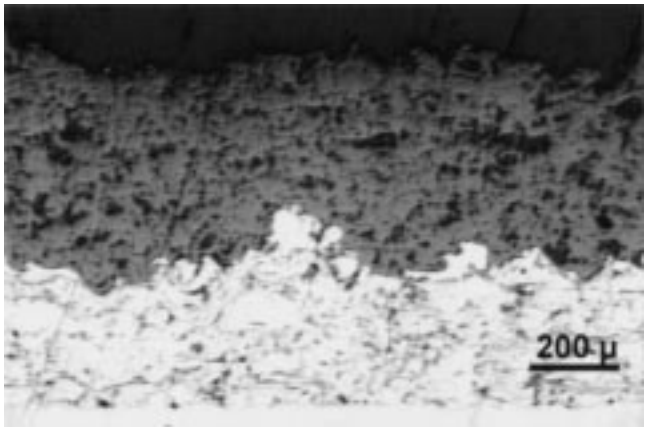

(b)

Fig. 4 Microstructure of TBCs sprayed under normal conditions: (**a**) surface and (**b**) cross-sectional views

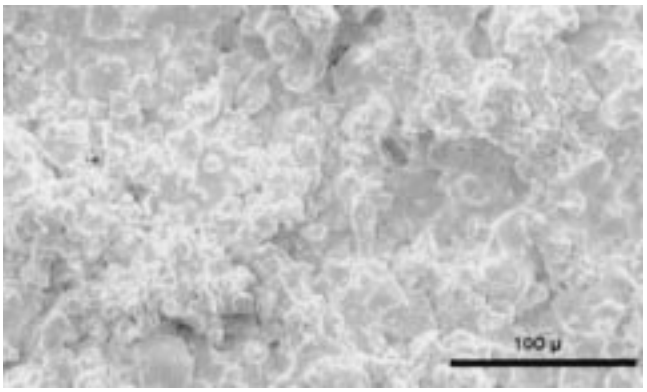

(a)

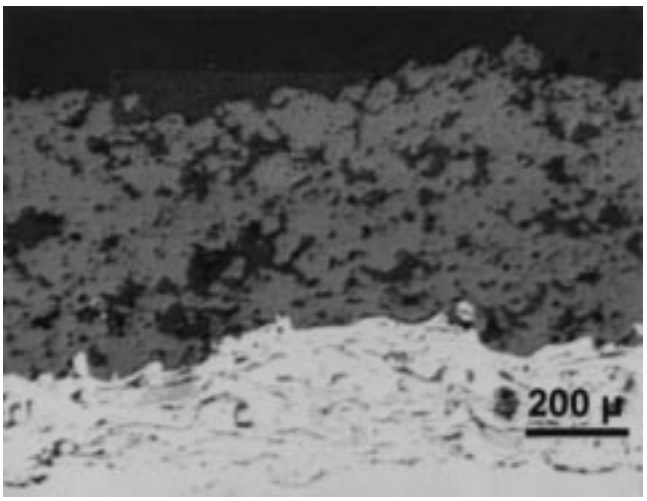

(b)

Fig. 5 Microstructure of the torch-too-close spraying condition. The top-coat layer is slightly more compact and there are large regions of well-bonded particles: (**a**) surface and (**b**) cross-sectional views

operating conditions will be taken as "model" coatings to which all others will be compared.

The characteristics of the model coatings were identified using SEM micrographs of the coating surface and optical micrographs taken in cross section. Figure 4 shows the microstructure from an as-sprayed coating processed under normal conditions. The cross-sectional view (b) shows the lamellar nature of the particles, which is best seen in the bond coat. Porosity is indicated by the arrows, and the inherent roughness of plasma-sprayed coatings is apparent. Some of the "porosity" in polished sections of these coatings arises from pullout of material during polishing. Figure 4(a) shows a typical surface view of the normal specimens. The features evident in this micrograph are a mixture of melted, partially melted, and unmelted particles, the roughness of the coating, and a small amount of intersplat cracking. The mixed-particle characteristics are common even though an optimum microstructure would consist only of entirely melted particles.

Figure 5 shows similar micrographs for the torch-too-close spraying condition. Notice in the surface view the increased proportion of melted splats. Some unmelted particles remain, which

are practically unavoidable in spraying high-melting-point ceramic powders. This spraying condition is the equivalent of increasing the effective temperature of the particles as they impinge upon the substrate. Models used in the literature indicate that by increasing the input current, or by decreasing the working distance between the torch and substrate, the porosity is decreased and the splats are better bonded, because more particles are deposited in the molten state. Additionally, the substrate reaches a higher temperature during deposition due to the proximity of the plasma flame. In relation to the mechanical models presented earlier, this as-sprayed condition provides improved mechanical bonding, but yields a higher residual stress due to larger temperature change.

The as-sprayed microstructure of the specimens with the bond coat too thin is quite a contrast to the previous two examples. The bond coat thickness is negligible if there is bond coat present at all (Fig. 6b). This yields a thermal expansion mismatch between the YSZ and the substrate, which is greater in this case than for the samples with a bond coat. As a result, there is an increased residual tensile stress during the quenching of the particle, compared to that of those particles deposited on a substrate with a bond coat. This is the cause of the more significant damage found in the microstructure. The intersplat crack network is well developed (Fig. 6a).

Finally, the coatings sprayed with the top coat too thick are quite similar to the normal coatings, as would be expected. These coatings are sprayed with the same parameters, except that more YSZ is deposited than usual. Micrographs typical of these coatings are shown in Fig. 7. Essentially, the only difference expected between these samples and the normal samples is the volume of the coating. More flaws are likely due to the increased volume, and a greater quantity of AE could be expected. This point will be discussed later.

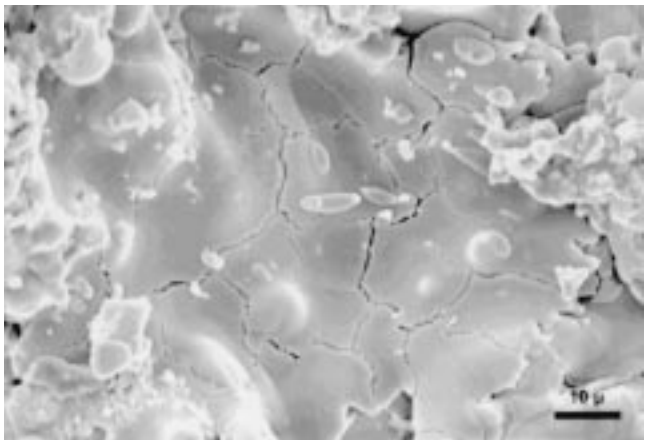

(a)

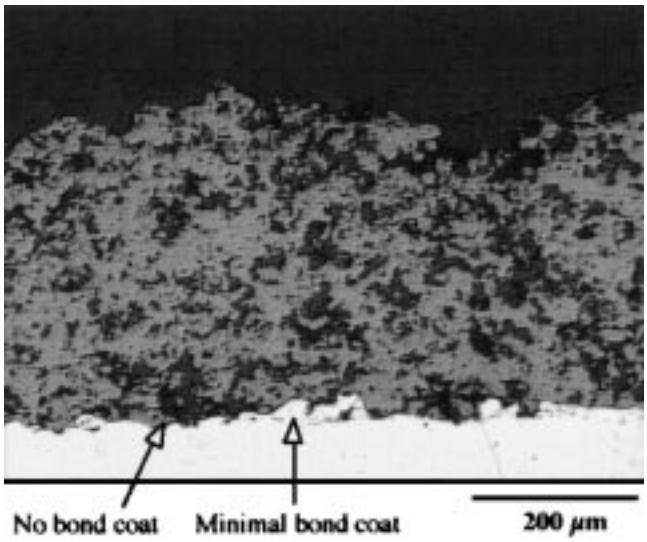

(b)

Fig. 6 Microstructure of a coating produced with the bond-coat-too-thin. (**a**) Surface view shows the highly cracked as-sprayed condition. (**b**) Cross section shows virtually nonexistent bond coat

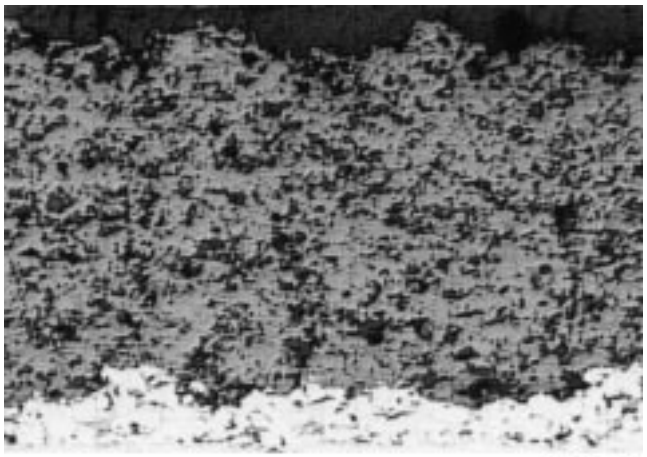

(a)

(b)

Fig. 7 (**a**) and (**b**)Microstructure for top-coat-too-thick condition. Except for the extra thickness, the coating should be the same as a normally deposited coating

3.2 AE Characterization

Trends in AE data are used to describe the dominant fracture mechanisms occurring in the microstructure. The data reduction procedures used in this work were the cumulative amplitude distribution modeled as a power-law function and the χ^2 and Student Newman-Keuls (SNK) range test statistical analyses. (Further details about these statistical tests are in the Appendix.) The other parameter that will be discussed briefly is the counts per hit of a group of samples. Additionally, the time dependency of AE events, both in a single thermal shock cycle and in the overall test (six cycles), was examined for distinguishable trends. These may be more pertinent in the context of a nondestructive test, since it would be favorable to have some kind of in-process indicators as guidelines for acceptance/rejection criteria, instead of post-test statistics.

The greatest proportion of the total emission over six thermal shock cycles, for every specimen, occurred in the first thermal shock cycle. This behavior can be attributed to the relief of residual stresses from the as-sprayed coatings. After the first cycle, there is at least an order-of-magnitude drop in AE counts during subsequent thermal shock cycles, as shown in Fig. 8. Due to the relatively low level of AE in cycles 2 to 6, the focus of the data analysis was placed on the emission occurring in the first thermal shock cycle. The consistency of this drop-off implies that the condition of the as-sprayed microstructure may be recognizable with AE data from just the first cycle.

3.2 Statistical Analysis

Two different statistical procedures were used in the data analyses. The mean and standard deviation of *b* values for each spraying condition were calculated using the raw data. General trends in each spraying condition could be established, but the scatter among samples in a group prevented any meaningful conclusions from being made. The standard deviation for each group (normal, gun-too-close, bond-coat-too-thin, top-coat-too-thick) was large, and the 95% confidence intervals had significant overlap. A statistical test for significant difference between means, the SNK range test, showed that the data contained too many outliers to be useful.[17] This is a direct result of the variability in plasma-sprayed coatings, which is commonplace.[18]

An example of the inconsistency common to thermal spray deposition is shown in Fig. 9. The micrographs shown are from a single metallographic specimen cut from a piston with a commercially applied TBC. They show a large difference in the

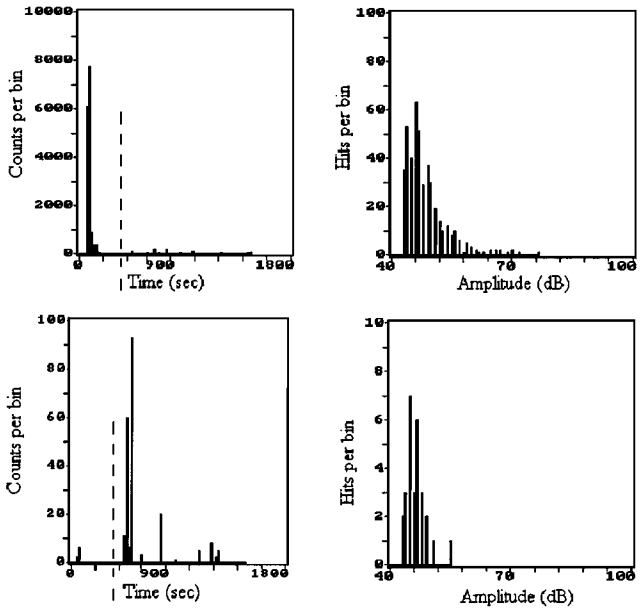

Fig. 8 Typical change in AE activity from the first thermal shock cycle to subsequent cycles. A change in scale on the Y-axis is necessary because of the large decrease in signal

(a)

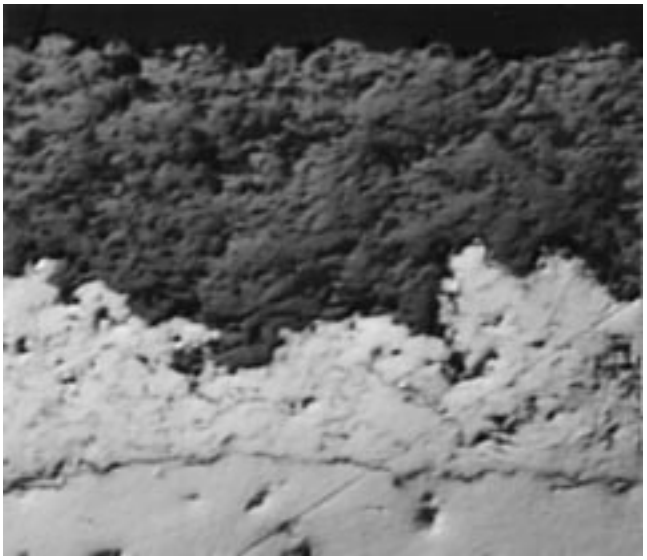

(b)

Fig. 9 (**a**) and (**b**)The large variation in plasma-sprayed coatings can be clearly seen in these micrographs. Both images are from the same metallographic sample less than 1 cm apart (The coating thickness is approximately 300 mm.)

thickness of the YSZ and the bond coat within a square centimeter. This kind of variation can cause the AE data from a sample in the normal groups to resemble bond-coat-too-thin samples more than normal samples, for example.

The second procedure, Chi Square statistics (χ^2), was used to identify anomalous specimens.[17] This is a common statistical technique used to test the significance of association between samples in each group. For this work, in most cases, the differences between the samples in the same group were much smaller than the differences between samples in different groups. Ten out of 51 samples were eliminated to have a confidence level of 95% in the groupings.

The remaining samples consisted of sets of 12, 9, 10, and 10 for the normal, torch-too-close, bond-coat-too-thin, and top-coat-too-thick conditions, respectively. Cumulative amplitude distributions were used to calculate the *b* parameter for individual samples. A counts-per-hit average was found by dividing the total hits by the total counts. The counts-per-hit averages overlap extensively, making this analysis of no use for the purposes of this study.

Figure 10 provides a summary of the data in terms of the *b* value. The scatter plots show a diamond for the distribution of data in each group. The middle line of the diamond represents the mean value for that group, and the extreme points along the ordinate are the bounds of a 95% confidence interval. The solid line at $b = 2.5$ across all the groups is the mean for the entire population. A range test was performed to check the significance of the difference between the means for each group. The diameter of the circles for each group is equivalent to the width of the 95% confidence interval. The *b* data for the normal and top-coat-too-thick groups are distributed about the population mean. Most of the bond-coat-too-thin data points are higher, while most of the gun-too-close data points are lower. This trend shows a distinction between the groups, which can be related to the microstructure.

4. Discussion

Explanation of the AE behavior witnessed in this study can be related to the as-sprayed stress state of the coatings. The residual stress from the deposition of the coating has two components. A quenching component is due to the spreading and rapid solidification as the particle impinges on the substrate. This gives rise to a stress component, which is always tensile. The second component comes from cooling of the composite system after the spraying ceases. When the thermal expansion coefficient of the coating is less than the thermal expansion coefficient of the substrate, the stress generated upon cooling will be compressive. The relative magnitude of this stress component depends on the maximum temperature of the substrate during deposition.

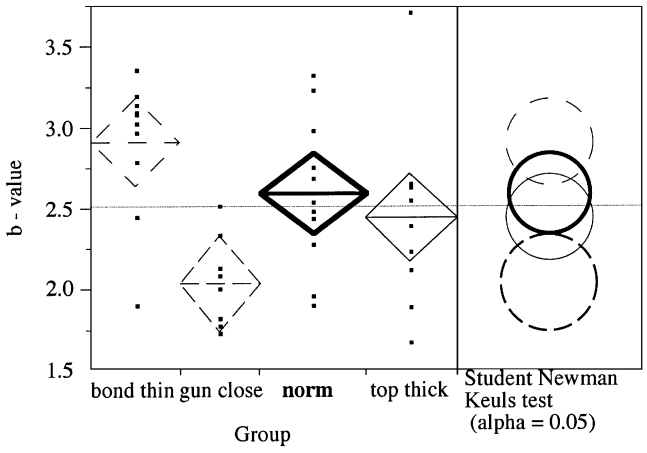

Fig. 10 A summary of the calculated *b* values after elimination of some samples using χ^2 statistics. The diamonds represent 95% confidence intervals. The circles on the right represent the 95% confidence intervals as calculated by the SNK range test

Every specimen in this experiment was sprayed with the substrate unheated and indicates that no additional heat was applied beyond the heat given off by the impinging particles. Qualitatively, the "steady-state" temperature of the substrate during the spray process will not be the same for each of the spraying conditions considered here. The substrate of the gun-too-close group will reach a higher temperature during deposition than the substrates of the other three groups. Hotter particles and a closer plasma flame are the reasons for the increase in temperature.

The higher the substrate temperature, the more the composite system will contract. This results in a higher compressive stress component. Combined with the tensile component (due to particle quenching), the effect will be a net residual stress, which is lower (even compressive above some critical substrate temperature) than it would be if the substrate were cooler. Additionally, there is a different bonding state for the gun-too-close group due to the higher proportion of fully molten particles. A greater percentage of the effective splat surface area is well bonded compared to other spraying conditions (Fig. 5). These factors combine to produce a microstructure that has fewer cracks in the as-sprayed condition.

The focus of the statistical analysis was on AE from the first thermal shock cycle. A large percentage of these AE events occurred during the upshock portion of the cycle while the coating was in tension. This was primarily due to relief of residual stresses and the initiation and growth of cracks. Figure 11 shows examples of this time-dependent behavior plotted as counts versus time. The transition from upshock to downshock is indicated by the dotted lines in each portion of the figure. This behavior is understandable, since crack growth in ceramics generally occurs under tensile stresses.

During the downshock part of the cycle, the coating is under a compressive load. One would expect fewer, if any, cracks to grow in compression. Therefore, the reduced number of AE events during this portion of the cycle is expected (Fig 11). In-plane compressive stresses have been found to produce significant tensile stresses perpendicular to the plane of the coating. These tensile stresses are the driving force for debonding.[7] However, such stresses arise due to surface curvature causing stress concentrations. Since these coating/substrate systems are flat, the generation of a through-thickness tensile stress is unlikely. Additionally, a much greater amount of AE would be expected during failure than that which is seen here. Explanations for these events include sliding particle as the coating contracts and the dislodging of loosely bound particles.

After the first thermal shock cycle, most of the AE occurred in the downshock portion of the cycle. Figure 11 shows evidence of this change, from a large amount of activity predominantly during upshock to very little during downshock for the first cycle (top left), with a reversal of this distribution for the second cycle

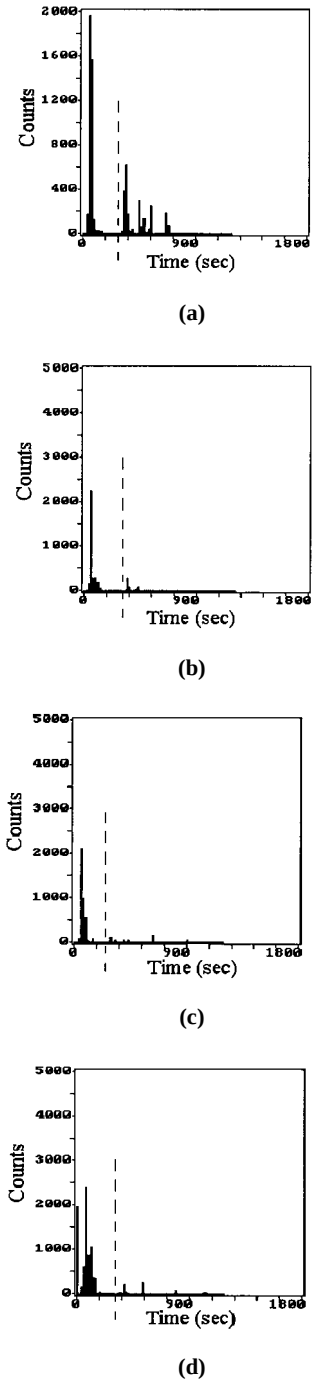

Fig. 11 (**a**) through (**d**)The time dependency of the AE counts for the first thermal shock cycle. This trend was independent of the spraying condition as shown here. The dotted line indicates the transition from upshock (0 to 300 s) to downshock (300 to 1200 s)

(bottom left). In some cases, the number of acoustic events was insignificant (< 5 hits) making it difficult to draw conclusions from the data. In general terms, the emission occurring at the same load levels can be significant, often interpreted to mean that serious cracks have been established. These cracks may be subject to slow crack growth, which reduces the fracture strength of the material. The long-term effect of this activity for these samples is unknown at this time. A possible source of these hits is the sliding of splats past each other as the coating contracts. This perturbation would be small, which is consistent with the low-amplitude hits. These AE events are relatively insignificant when compared to the amount of activity measured in the first cycle.

The data analysis given in Fig. 10 shows that distinctions in AE characteristics in terms of the *b* parameter are possible. This plot shows the 95% confidence intervals, as indicated by the diamonds fitted to each scatter plot. Also shown by the overlapping circles on the right of the figure is the result of an SNK range test for significant differences between means. The greater the overlap, the less significant is the difference between means.

The mean values of the normal and top-coat-too-thick groups are very close. The result is a large overlap in the 95% confidence interval for these two groups. This similarity is understandable, since coatings from both groups were sprayed with the same parameters except for coating thickness. The additional volume of the coating in the top-coat-too-thick group increased the chance of having larger flaws present, which probably accounts for the shift to slightly lower *b* values.

More significant distinctions can be made when comparing the data of the torch-too-close group to the other three groups. There was a trend for lower *b* values in this group, which can be explained by considering the microstructure. During deposition, more particles were in a fully molten state, which promoted improved interparticle cohesion during deposition and decreased porosity. The bonding between splats is much better in this case. Also, there are fewer cracks present in the as-sprayed condition than for the other sample groups (Fig. 5a). This suggests that, initially, there are fewer microcracks to arrest interlamellar crack propagation. Upon thermal-shock loading, cracks are likely to propagate farther without being arrested. This would result in a corresponding increase in energy released, yielding larger amplitude AE events (smaller *b* values).

The SNK range test shows the significance of the difference between the gun-too-close samples and the remaining groups. With a 95% confidence interval, there is no overlap with the data from the normal specimens. This is important, because it suggests that samples that have a *b* value less than about 2.25 are significantly different and should be rejected. There are two data points in the normal group below this value, which can only be attributed to the variability in the spraying process that has already been discussed. Alternative data evaluations, such as the shape of the cumulative amplitude distribution, may distinguish these as atypical samples. The confidence interval of the bond-coat-too-thin group has a slight overlap with the normal and the thick-top-coat groups and is significantly different from the bond-coat-too-thin sample sets. The overlap with the normal group is eliminated if the confidence interval is decreased to 93%.

The higher *b* values seen in the bond-coat-too-thin group can also be explained by considering the as-sprayed microstructure. More significant cracking is present in these coatings (Fig. 6a). Cracks that propagate through this microstructure are more likely to be arrested after propagating for one splat diameter. This effectively limits the energy that can be released from the structure. The high proportion of low-amplitude hits that are seen in the data (high *b* values) supports this model.

5. Summary and Conclusions

The AE response of plasma-sprayed TBCs was evaluated for coatings sprayed under a variety of conditions at a commercial facility. The samples were sprayed under normal operating conditions and three other conditions (the plasma gun-too-close to the substrate, the bond-coat-too-thin, and the top-coat-too-thick).

Each sample was cycled from room temperature to 1000 °C in a tube furnace. Acoustic emission was monitored during the upshock and downshock portions of six thermal shock cycles. It was found that there was at least an order of magnitude drop in acoustic events from the first thermal shock cycle to subsequent cycles. Based on this observation, it was proposed that the activity in the first cycle was critical and that the condition of the microstructure could be related to this activity.

The χ^2 test of significance is useful for limiting the scatter in the data by eliminating rogue samples, which are uncharacteristic for the groups in which they were processed. The calculated *b* value from the power-law fit of the cumulative amplitude distribution function can be related to the condition of the as-sprayed microstructure of the TBC.

Significant differences in the acoustic response between sample groups were seen in the data from the first thermal shock cycle. Since the test is short and the data can be handled easily by a microprocessor, development of a quality control test using AE is quite feasible.

Appendix

A.1 AE Spectroscopy

The prevailing features of an AE waveform are hits, amplitude, ringdown counts, energy, and duration. A schematic waveform is shown in Fig. 12 as a reference. The most influential parameter in this figure is the threshold setting. The threshold is a user-defined gate such that only signals with peak amplitudes greater than the threshold are counted as AE events. It is a measure of the sensitivity of the test and may be set to eliminate white noise and other background interference. A higher threshold yields fewer spurious events and has a low sensitivity, whereas a low threshold allows many more signals to be registered. The threshold setting in this work (43 dB) is considered to be an intermediate sensitivity.[9] This value was chosen experimentally, by decreasing the threshold as far as possible while still excluding the extraneous noises.

A hit is defined by the entire waveform of the signal measured between the first threshold crossing and the last threshold crossing. Amplitude is defined as the height of the strongest peak in the waveform. Ringdown counts are the number of times the signal crosses the preset threshold for a given hit. Energy is the total energy from the ringdown counts and is measured by the area under the rectified signal envelope, *i.e.*, the dotted line in the figure. Duration is the amount of time needed for a given signal to decay below the threshold setting.

The two AE parameters chosen for this study were amplitude distribution and hits/count. Both are considered to be crack specific but not thickness dependent.[9]

The experimental setup was a commercial unit available from Physical Acoustics Corp. (Princeton, NJ). The D9215 sensor is

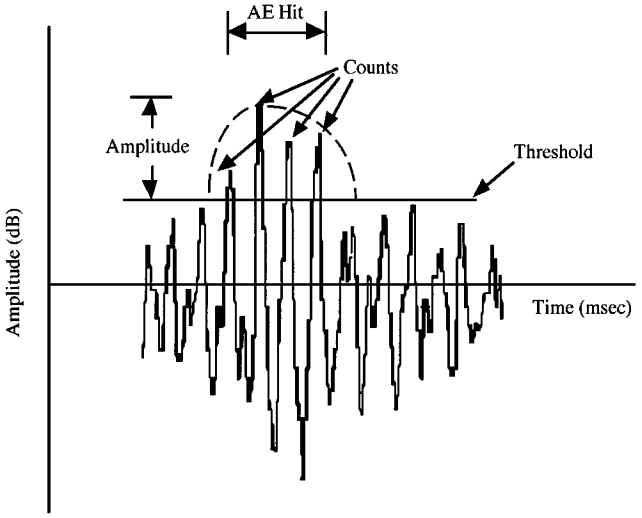

Fig. 12 Characteristics of an AE waveform

a resonant-type transducer with a primary frequency of 85 kHz. Consequently, a 100 to 400 kHz bandpass front-end filter was established to read only the lower frequency hits. This allowed elimination of white noise, which was found to occur at an average frequency of approximately 1000 kHz. The operating parameters included a 60 dB preamplification, a system gain of 20 dB, and a threshold setting of 43 dB. A Hit Definition Time of 1000 μs and a Hit Lockout Time of 300 μs were chosen to optimize this particular signal: a ceramic coating producing stress waves that propagate through a metallic substrate. (A PAC[18] AEDSP-32/16 processor for the MISTRAS-2001 system was used to collect and process the data, PAC GRAFPLUS software was used for image processing upon data replay along with the ATASC, ATTO, and MI-POST PAC utilities for data formatting and post-test filtering.)

A.2 Statistical Analyses

The SNK range test is the equivalent of the Student *t*-test for multiple means. Several range tests exist and give comparable analyses when used to decide the significance of differences between multiple means. The range tests all take into consideration the number of specimens in a group and the standard deviation.

Similarly, the χ^2 test is a common procedure used to distinguish the significance of association between members of a set. Using an accepted statistical procedure provides an objective, reproducible method to eliminate outliers. The χ^2 test was performed using the Null Hypothesis that the samples in the group had similar characteristics. If the χ^2 analysis showed that there were real differences in the samples, then individual samples were systematically eliminated, and the calculation was performed again. The criterion for acceptance of the Null Hypothesis was a probability of occurrence of 5% ($\alpha < 0.05$). This condition would mean that the differences between samples in a given group are due to random error. If $\alpha < 0.05$, the samples were taken as being significantly different, or the differences were not due to chance. Using this approach, a handful of speci-

mens were discarded as being atypical of the spraying condition under which they were processed.

References

1. N. Ravi Shankar, C.C. Berndt, H. Herman, and S. Rangaswamy: *Am. Ceramic Soc. Bull.* 1983, vol. 62 (5), pp. 614-19.
2. C.C. Berndt *et al.: J. Thermal Spray Technol.,* 1992, pp. 341-56.
3. W.J. Lackey, D.P. Stinton, G.A. Cerny, L.L. Fehrenbacher, and A.C. Schaffhauser: "Ceramic Coatings for Heat Engine Materials—Status and Future Needs," ORNL/TM-8959, Oak Ridge National Laboratory, Oak Ridge, TN 1984.
4. S. Kuroda and T.W. Clyne: *Thin Solid Films,* 1991, vol. 200, pp. 49-66.
5. R. Tucker: "Advanced Thermal Spray Deposition Techniques," ASM chapter of Western New York (presented at a short course at Alfred University, Alfred, NY, 1996).
6. S.C. Gill and T.W. Clyne: in *High Performance Ceramic Films and Coatings,* P. Vincenzini, ed., Elsevier Science Publishers, New York, NY, 1991, pp. 339-52.
7. D.L. Ruckle: *Thin Solid Films,* 1980, vol. 73, pp. 455-61.
8. Y. Hinton: *ASTM Standardization News,* Jan. 1995, pp. 36-39.
9. A.A. Pollock: *Practical Guide to Acoustic Emission Testing,* Physical Acoustics Corp., Princeton, NJ, 1988.
10. *Acoustic Emission (Nondestructive Testing Monographs and Tracts, Vol. 2),* James R. Matthews, ed., Gordon and Breach Science Publishers, New York, NY, 1983.
11. K.J. Konsztowicz and D. Fontaine: *J. Nondestr. Eval.,* 1989, vol. 8 (1), pp. 1-12.
12. K.J. Konsztowicz: *J. Am. Ceramic Soc.,* 1990, vol. 73 (3), pp. 502-08.
13. C.C. Berndt and H. Herman: *Thin Solid Films,* 1983, vol. 108, pp. 427-37.
14. A.A. Pollock: *Int. Adv. Nondestr. Testing,* 1981, vol. 7, pp. 215-39.
15. D. Almond, M. Moghisi, and H. Reiter: *Thin Solid Films,* 1983, vol. 108, pp. 439-47.
16. A.A. Pollock: *2nd Conf. on Acoustic Emission/Microseismic Activity in Geologic Structures and Materials,* Trans Tech Publications, Rockport, ME, 1980, pp. 400-21.
17. M.J. Moroney: *Facts from Figures,* Penguin Books, Baltimore, MD, 1963, pp. 246-70.
18. S.W. Winn: Bachelor's Thesis, Scholes Library, NYS College of Ceramics, Alfred University, Alfred, NY, to be published.